

FEATURED ARTICLES

## Advanced Manufacturing of Intermediate-Temperature Protonic Ceramic Electrochemical Cells

To cite this article: Shenglong Mu *et al* 2020 *Electrochem. Soc. Interface* **29** 67

View the [article online](#) for updates and enhancements.



**240th ECS Meeting** ORLANDO, FL

Orange County Convention Center **Oct 10-14, 2021**



Abstract submission due: April 9

**SUBMIT NOW**

# FUTURE ECS MEETINGS



**239th ECS Meeting**  
with the  
**18th International Meeting  
on Chemical Sensors**  
CHICAGO, IL  
May 30-June 3, 2021  
*Hilton Chicago*



**240th ECS Meeting**  
ORLANDO, FL  
October 10-14, 2021  
*Orange County Convention Center*



**241st ECS Meeting**  
VANCOUVER, BC, CANADA  
May 29-June 2, 2022  
*Vancouver Convention Center*



**242nd ECS Meeting**  
ATLANTA, GA  
Oct. 9-13, 2022  
*Atlanta Hilton*



[www.electrochem.org/meetings](http://www.electrochem.org/meetings)

# Advanced Manufacturing of Intermediate-Temperature Protonic Ceramic Electrochemical Cells

by Shenglong Mu, Zeyu Zhao, Hua Huang, Jincheng Lei, Fei Peng, Hai Xiao, Kyle S. Brinkman, and Jianhua (Joshua) Tong

## Introduction

Proton conducting oxide (i.e., protonic ceramic) has been thought of as an ideal solid electrolyte for energy conversion and storage applications since Iwahara et al. reported the perovskite-type protonic ceramics represented by doped barium/strontium cerates and zirconates in the 1980s.<sup>1,2</sup> Proton, as the charge carrier in protonic ceramics, possesses a much lower transport activation energy than oxide-ion, which has rendered protonic ceramics for extensive intermediate-temperature (IT, 400-700°C) electrochemical devices such as protonic ceramic fuel cells (PCFCs),<sup>3-7</sup> reversible protonic ceramic fuel cells,<sup>8-10</sup> and protonic ceramic membrane reactors.<sup>11</sup>

In the past four decades, significant effort has focused on discovering high-performance new protonic ceramic materials simultaneously possessing high proton conductivity and good chemical stability.<sup>12-17</sup> On one hand, doped barium cerate perovskite oxides usually showed high proton conductivity at intermediate temperatures. For example,  $\text{BaCe}_{0.8}\text{Gd}_{0.2}\text{O}_{3-\delta}$  showed a proton conductivity as high as  $5 \times 10^{-2}$  S/cm at 600°C<sup>18</sup>. However, low chemical stability under carbon dioxide and water vapor atmospheres ruled out the practical applications of doped barium cerate materials. On the other hand, doped barium zirconates (e.g.,  $\text{BaZr}_{0.8}\text{Y}_{0.2}\text{O}_{3-\delta}$ ) showed excellent chemical stability under the same atmospheres, whose proton conductivity, however, usually was much lower than their counterparts of doped barium cerates.<sup>19</sup> The recent discovery indicated that the phase-pure solutions formed from doped barium cerates and doped barium zirconates (e.g.,  $\text{BaCe}_{1-x-y}\text{Zr}_x\text{Y}_y\text{O}_{3-\delta}$  (BCZY)<sup>20-22</sup>,  $\text{BaCe}_{0.7}\text{Zr}_{0.1}\text{Y}_{0.1}\text{Yb}_{0.1}\text{O}_{3-\delta}$  (BCZYYb7111))<sup>4</sup>,  $\text{BaCe}_{0.4}\text{Zr}_{0.4}\text{Y}_{0.1}\text{Yb}_{0.1}\text{O}_{3-\delta}$  (BCZYYb4411))<sup>5</sup> successfully combined the high proton conductivity from doped barium cerates and the high chemical stability from doped barium zirconates together. The BCZY and doped BCZY perovskite oxides showed a compromised performance of good conductivity and improved stability and became the state-of-the-art protonic ceramic materials, which have been extensively used for the protonic ceramic electrochemical cells (PCECCs).

While pursuing high-performance protonic ceramic materials, the proton conductivities for the same nominal compositions always showed a vast distribution according to the reports from different groups. This proton conductivity discrepancy became worse for the protonic ceramic materials with higher zirconium amounts in the perovskite oxide structure. For example, the summary of the proton conductivity for the typical protonic ceramic material of  $\text{BaZr}_{0.8}\text{Y}_{0.2}\text{O}_{3-\delta}$  (BZY20)<sup>23-32</sup> (Fig. 1) showed that the conductivities broadly distribute in the range of  $10^{-5}$ -1 S/cm, which has almost five orders of magnitude difference. The well-accepted reasons for the conductivity discrepancy are the poor control of the microstructure (e.g., low relative density, small grain size, and impurities precipitated in the grain boundary regions) and the significant barium loss (e.g., barium dissolution to solvent during powder processing and barium evaporation during high-temperature firing) for the fabricated protonic ceramic parts due to the high firing temperatures intrinsically required by the refractory nature of the barium zirconate-based materials. Therefore, in addition to the discovery of high-performance protonic ceramic materials, the manufacturing of the

state-of-the-art protonic ceramic materials into protonic ceramic parts (e.g., thin films) to achieve the desired microstructures for ensuring the stable high proton conductivity has been playing a decisive role for the practical application of protonic ceramics to energy conversion and storage devices.

In this work, we will first summarize the conventional sintering methods for the manufacturing of protonic ceramics. After that, we will briefly review the state-of-the-art solid state reactive sintering (SSRS) method, which has found extensive applications for manufacturing the button cells to demonstrate the performance of the versatile PCECCs. Then, we will introduce the newest technique of rapid laser reactive sintering (RLRS) for fast and cost-effective sintering of protonic ceramics, which provides the possibility to manufacture PCECC stacks using additive manufacturing rapidly. Finally, we will briefly introduce the development of integrated additive manufacturing and laser processing (I-AMLPLP) technique to manufacture protonic ceramics.

## Conventional Sintering Methods

Many fabrication efforts have been pursued over decades to achieve protonic ceramic parts (e.g., pellets and thin films) with high relative density and desired microstructures. The conventional ceramic processing method of solid state sintering of shaped parts from solid state reaction derived phase-pure protonic ceramic powders usually need sintering temperatures higher than 1,700-1,800°C and sintering time longer than 10h to achieve the required

(continued on next page)

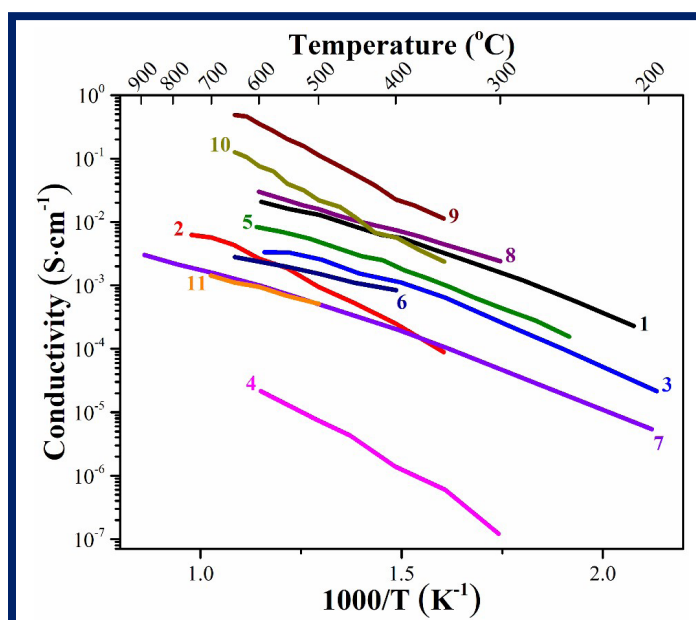


Fig. 1. Summary of some proton conductivity data for the typical protonic ceramic BZY20 fabricated by different methods in different research groups. The data for plots of 1-11 came from References 23-32 respectively.

relative density, which, however, inevitably resulted in severe barium loss and low proton conductivity.<sup>20</sup> The two-step sintering method, typically consisting of a high-temperature sintering step for a short time (few minutes) to achieve critical density and a followed low-temperature sintering step for a long time to fulfill the desired grain growth, improved the microstructure of proton ceramics and achieved decent proton conductivity. However, the two-step sintering method still could not coherently avoid the high sintering temperatures and extended sintering time.<sup>33</sup> The protection by using pure oxygen and complicated powder (mixture of barium carbonate and protonic ceramic powders) bath and using wet-chemistry derived high-quality phase-phase protonic ceramic powder are effective methods to prepare dense protonic ceramic pellets with high relative density and increased grain size, which, however, still required a sintering temperature higher than 1,600°C and sintering time longer than 20h.<sup>31</sup> The spark plasma sintering (SPS) technique was a powerful tool to achieve high ceramic relative density while limiting the grain size growth.<sup>34</sup> The SPS method usually resulted in high relative densities for protonic ceramic pellets, which showed a comparable proton conductivity to the samples obtained from the conventional sintering method. However, the SPS tool is still confronting equipment complexity, high cost, and limitation of sample geometries, making it challenging to utilize for the manufacturing of protonic ceramic devices practically. The pulsed laser deposition (PLD) technique showed the capability to achieve dense epitaxial thin films and demonstrated the high proton conductivity and promising fuel cell performance.<sup>30</sup> However, the PLD technique needs to address similar challenges as the SPS technique before its practical application.

Therefore, it is not hard to figure out that most of the sintering methods mentioned above are not so useful for the fabrication of PCECCs comprised of the anode, electrolyte, and cathode layers because of the high temperature, long time, or equipment complexity or limitation, and difficulty to integrate with conventional ceramic shaping techniques such as tape casting, screen printing, and extrusion.

## Solid State Reactive Sintering

In 2005, Haile et al. reported adding some specific transition metal oxides (e.g., ZnO, NiO, CuO) to phase-pure  $\text{BaZr}_{0.85}\text{Y}_{0.15}\text{O}_{3-\delta}$  (BZY15) synthesized by the combustion method achieved relative densities higher than 90% at 1,300°C, which were 300–400°C lower than the conventional densification for barium zirconate-based protonic ceramics.<sup>35</sup> After that, doped barium cerates and zirconates perovskite-type protonic ceramics showed improved sinterability while adding ZnO as an extra sintering aid or a component of the perovskite structure.<sup>21, 25, 36</sup> Inspired by this pioneering work related to improving sinterability for phase-pure perovskite-type protonic ceramics by ZnO, in 2010, Tong et al. developed the solid state reactive sintering (SSRS) method for sintering protonic ceramics at moderate temperatures (<1,500°C) directly from cost-effective raw materials of carbonates and single metal oxides.<sup>37</sup> With the fabrication of BZY20 as an example, Fig. 2 schematically describes the SSRS processes. The SSRS consisted of ball milling of the raw material precursor mixture, dry pressing of green pellets, and

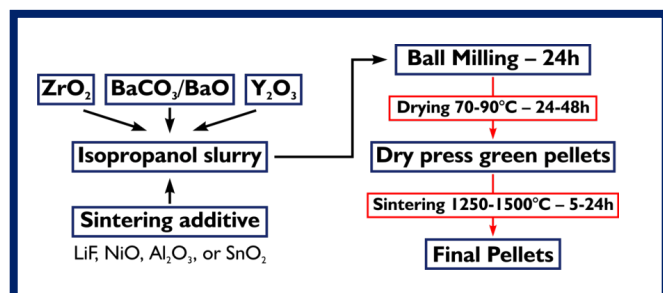


Fig. 2. Schematic description of solid state reactive sintering (SSRS) procedure with the fabrication of BZY20 pellets as an example.

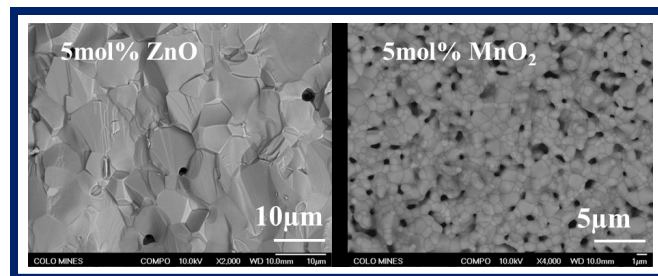


Fig. 3. SEM images of the fractured cross-sections of  $\text{BaCe}_{0.6}\text{Zr}_{0.3}\text{Y}_{0.1}\text{O}_{3-\delta}$  (BCZY63) pellets were fabricated by using the SSRS method at 1,450°C for 12h with ZnO and  $\text{MnO}_2$  as sintering aids. (Adapted from Fig. 3 in Reference 39 with copyright permission.)

moderate-temperature sintering of green pellets to achieve final sintered pellets. With the help of a small amount of sintering aid (e.g., NiO), the SSRS method combined the phase formation, pellet densification, and grain growth into a single moderate-temperature sintering step. The SSRS method then showed success for most of the popular perovskite-type protonic ceramic materials of yttrium doped barium cerate ( $\text{BaCe}_{0.8}\text{Y}_{0.2}\text{O}_{3-\delta}$ )<sup>38</sup>, yttrium-doped zirconates (e.g.,  $\text{BaZr}_{0.9}\text{Y}_{0.1}\text{O}_{3-\delta}$ )<sup>39</sup>, yttrium doped barium cerate and zirconate (e.g.,  $\text{BaCe}_{0.6}\text{Zr}_{0.3}\text{Y}_{0.1}\text{O}_{3-\delta}$ )<sup>39</sup>,  $\text{BaCe}_{0.2}\text{Zr}_{0.7}\text{Y}_{0.1}\text{O}_{3-\delta}$ <sup>40</sup>, and ytterbium and yttrium co-doped barium cerate and zirconate ( $\text{BaCe}_{0.7}\text{Zr}_{0.1}\text{Y}_{0.1}\text{Yb}_{0.1}\text{O}_{3-\delta}$ ).<sup>41</sup> The further mechanism study by Tong et al. indicated that the intermediate phase (e.g.,  $\text{BaY}_2\text{NiO}_3$ ) formed between the sintering aid single metal oxide and the proton components introduced a partial liquid sintering became the main reason for lowering the sintering temperature of protonic ceramics. The screening of 15 single metal oxides as sintering aids for  $\text{BaCe}_{0.6}\text{Zr}_{0.3}\text{Y}_{0.1}\text{O}_{3-\delta}$ <sup>39</sup> showed that single metal oxides could form a solution with  $\text{BaZrO}_3$  and introduce a large amount of oxygen vacancy and electronic conductivity, which could work as useful sintering aids (e.g., NiO, ZnO, CuO, and CoO). This screening also proved that the sintering aids of  $\text{Fe}_2\text{O}_3$  and  $\text{MnO}_2$  could partially sinter the protonic ceramics, which could manufacture porous protonic ceramic scaffolds. Therefore, as described in Fig. 3, the SSRS method could not only achieve fully densified and large-grained electrolytes but also could achieve a porous electrode scaffold with the desired porosity and small grain size.

Recently, Tong et al. also demonstrated the cost-effective and facile fabrication of PCFCs by the SSRS method.<sup>3</sup> As indicated in Fig. 4, the SSRS method could fabricate half cells consisting of anode support and electrolyte thin film, and single cells consisting of anode support, electrolyte thin film, and cathode scaffold thin layer by adjusting different kinds of sintering aids or poreformers. The SSRS significantly simplified the fabrication process for the manufacturing of PCFCs from cost-effective raw materials. The PCFCs fabricated by the SSRS method showed peak power density higher than 450mW/cm<sup>2</sup> at 500°C and stable operation longer than 1,100 h. After this successful device performance demonstration, the SSRS method has shown extensive successes for PCECCs, such as PCFCs, PCECs, protonic ceramic membrane reactors, reversible PCFCs, and solid state ammonia synthesis. Table 1 summarizes several representative applications that utilized the SSRS method to fabricate the whole or a part of the devices and the representative performance.<sup>3, 7, 42-49</sup>

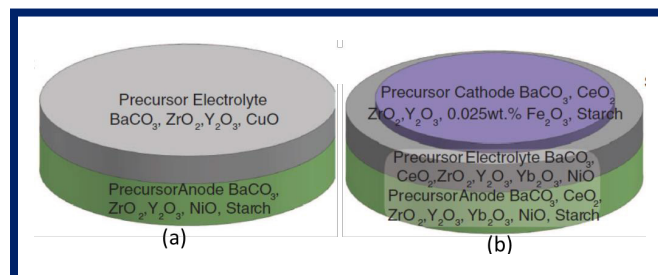


Fig. 4. Schematic description of the fabrication of (a) protonic ceramic half cells  $\text{BCZYYb}+\text{NiO}$  anode |  $\text{BCZYYb}$  electrolyte and (b) single cells  $\text{BCZYYb}+\text{NiO}$  anode |  $\text{BCZYYb}$  electrolyte |  $\text{BCZY63}$  cathode scaffold by using the SSRS method. (Adapted from Fig. 2b and Fig. 2c in Reference 3 with copyright permission.)

Table I. Summary of some representative performance for PCECCs fabricated by SSRS.			
Classes	Sintered Materials	Properties	References
Pure Materials	$\text{BaCe}_{0.4}\text{Zr}_{0.5}\text{Y}_{0.1}\text{O}_{3-\delta}$	$6.08 \times 10^{-3}$ S/cm	42
	$\text{BaZr}_{0.5}\text{Ce}_{0.3}\text{Y}_{0.2}\text{O}_{3-\delta}$	$2.50 \times 10^{-2}$ S/cm	43
	$\text{BaZr}_{0.5}\text{Ce}_{0.3}\text{Dy}_{0.2}\text{O}_{3-\delta}$	$4.30 \times 10^{-2}$ S/cm	43
	$\text{BaZr}_{0.84}\text{Y}_{0.15}\text{Cu}_{0.01}\text{O}_{3-\delta}$	$\sim 1.78 \times 10^{-2}$ S/cm	44
PCFCs	$\text{BaCe}_{0.7}\text{Zr}_{0.1}\text{Y}_{0.1}\text{Yb}_{0.1}\text{O}_{3-\delta}$	$\sim 650$ mW/cm <sup>2</sup>	3
	$\text{BaCe}_{0.7}\text{Zr}_{0.1}\text{Y}_{0.1}\text{Sm}_{0.1}\text{O}_{3-\delta}$	410 mW/cm <sup>2</sup>	45
	$\text{BaZr}_{0.8}\text{Y}_{0.2}\text{O}_{3-\delta}$	660 mW/cm <sup>2</sup>	7
	$\text{BaCe}_{0.7}\text{Zr}_{0.1}\text{Y}_{0.1}\text{Yb}_{0.1}\text{O}_{3-\delta}$	237 mW/cm <sup>2</sup>	46
Hydrogen Permeation Membranes	$\text{BaZr}_{0.80}\text{Y}_{0.15}\text{Mn}_{0.05}\text{O}_{3-\delta}$	0.8 mL/min <sup>-1</sup> cm <sup>-2</sup> (1000°C)	47
	$\text{BaZr}_{0.8}\text{Y}_{0.2}\text{O}_{3-\delta}$	$4.3 \times 10^{-8}$ mol cm <sup>-2</sup> s <sup>-1</sup> (900°C)	48
	$\text{BaCe}_{0.8}\text{Y}_{0.2}\text{O}_{3-\delta} - \text{Ce}_{0.8}\text{Y}_{0.2}\text{O}_{2-\delta}$	0.0744 mL min <sup>-1</sup> cm <sup>-2</sup> (900°C)	49

Therefore, we can conclude that SSRS is the state-of-the-art sintering method for the manufacturing of PCECCs cost effectively. However, the cofiring of anode and electrolyte can still not independently optimize the electrolyte and electrode microstructures. The long-term furnace sintering still cannot satisfy the rapid consolidation of each layer for additive manufacturing. Furthermore, the sintering aid effect and the sintering mechanism need us to contribute more effort to achieve further progress of SSRS for commercial applications to manufacturing large-scale PCECCs.

## Rapid Laser Reactive Sintering

Although the SSRS technique has demonstrated great success for the fabrication of PCECCs, the long-term (>10h) cofiring of the electrolyte and electrode (e.g., anode cermet) at a high temperature (>1,400°C) is still an inevitable step, which makes the independent optimization of the component layers (e.g., dense and large-grained electrolyte and nanoporous electrode) impossible. Furthermore, the manufacturing of PCECC stacks has to follow complicated procedures: fabrication of half cells consisting of anode support and electrolyte thin film, cofiring of half cells, deposition of the cathode, firing the cathode, and assembly of self-supported thick single cells, which not only make it impossible to achieve high volumetric power density but also make the manufacturing complicated and expensive.

In their most recent work, Tong et al. at Clemson University developed a so-called rapid laser reactive sintering (RLRS) method for fast processing protonic ceramics with the desired crystal structures, microstructures, and geometries.<sup>50-53</sup> As schematically described in Fig. 5, the RLRS process consists of the preparation of printable paste from component raw materials (carbonate and single metal oxides) mixed with sintering aid, the deposition of a thin green film of the targeted protonic ceramics, and the reactive sintering by rapid CO<sub>2</sub> laser scanning. Like the SSRS, the phase formation, densification, and grain growth for achieving protonic ceramic electrolyte thin films could integrate into a single laser sintering step. However, the RLRS method has several apparent advantages over

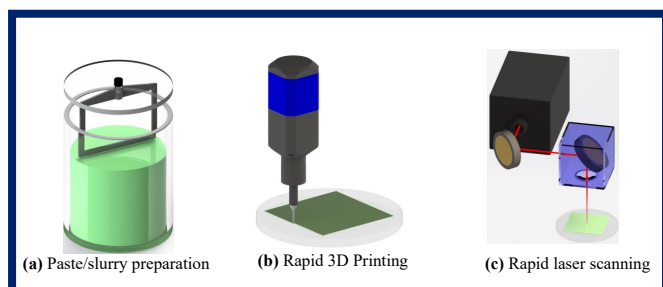


Fig. 5. Schematic description of the rapid laser reactive sintering (RLRS) process. (Adapted from Fig. 1 (Route 2) in Reference 51 (open access).)

the SSRS: short processing time (seconds/minutes versus several hours), selectively sintering of pre-programmed regions allowing independent processing of different component layer, and easy controlling of microstructures (grain boundary-free and epitaxially grown dense electrolyte thin films and nanoporous electrodes or electrode scaffolds) by adjusting laser operation parameters and sintering aids.

Tong et al. extensively applied the RLRS technique for processing the state-of-the-art protonic ceramics: dense electrolytes (BCZYYb+1wt%NiO, BCZYYb, BZY20+1wt%NiO, and BZY20), porous electrodes/electrode scaffolds (40wt% BCZYYb+60wt%NiO, BaCo<sub>0.4</sub>Fe<sub>0.4</sub>Zr<sub>0.1</sub>Y<sub>0.1</sub>O<sub>3-δ</sub> (BCFZY0.1), BaCe<sub>0.6</sub>Zr<sub>0.3</sub>Y<sub>0.1</sub>O<sub>3-δ</sub> (BCZY63)), dense interconnect (La<sub>0.7</sub>Sr<sub>0.3</sub>CrO<sub>3-δ</sub>/LSC), and dense mixed protonic and electronic-conduction composite (BaCe<sub>0.85</sub>Fe<sub>0.15</sub>O<sub>3-δ</sub>-BaCe<sub>0.15</sub>Fe<sub>0.85</sub>O<sub>3-δ</sub>/BCF).<sup>51</sup> Figure 6<sup>51</sup> summarizes the XRD patterns for the protonic ceramic thin films prepared by the RLRS. All the protonic ceramics achieved the desired crystal structures. The electrolyte, interconnector, cathode scaffold, and cathode all achieved phase-pure perovskite structures, same as those obtained by the conventional furnace sintering method. The XRD patterns for anode included the perovskite and nickel oxide phase without any other impure phases. Even the complicated dual perovskite hydrogen-permeable membrane consisting of two different perovskite phases (BaCe<sub>0.85</sub>Fe<sub>0.15</sub>O<sub>3-δ</sub>-BaCe<sub>0.15</sub>Fe<sub>0.85</sub>O<sub>3-δ</sub>) was successfully achieved by the RLRS method. Figure 7<sup>51</sup> summarizes the SEM images of

(continued on next page)

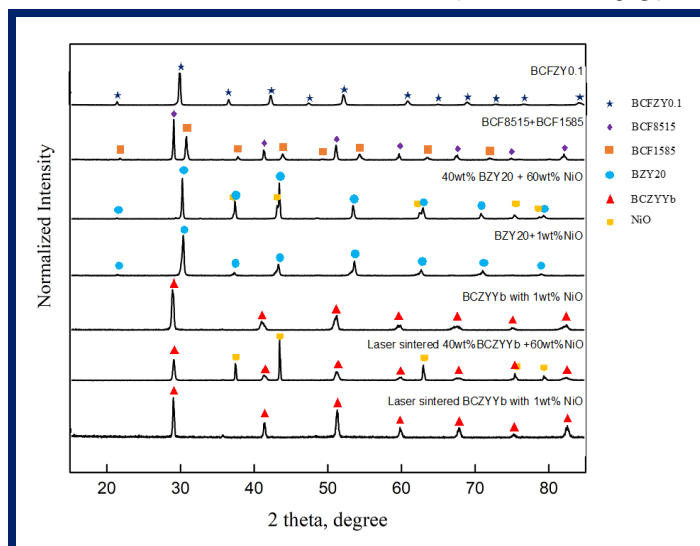
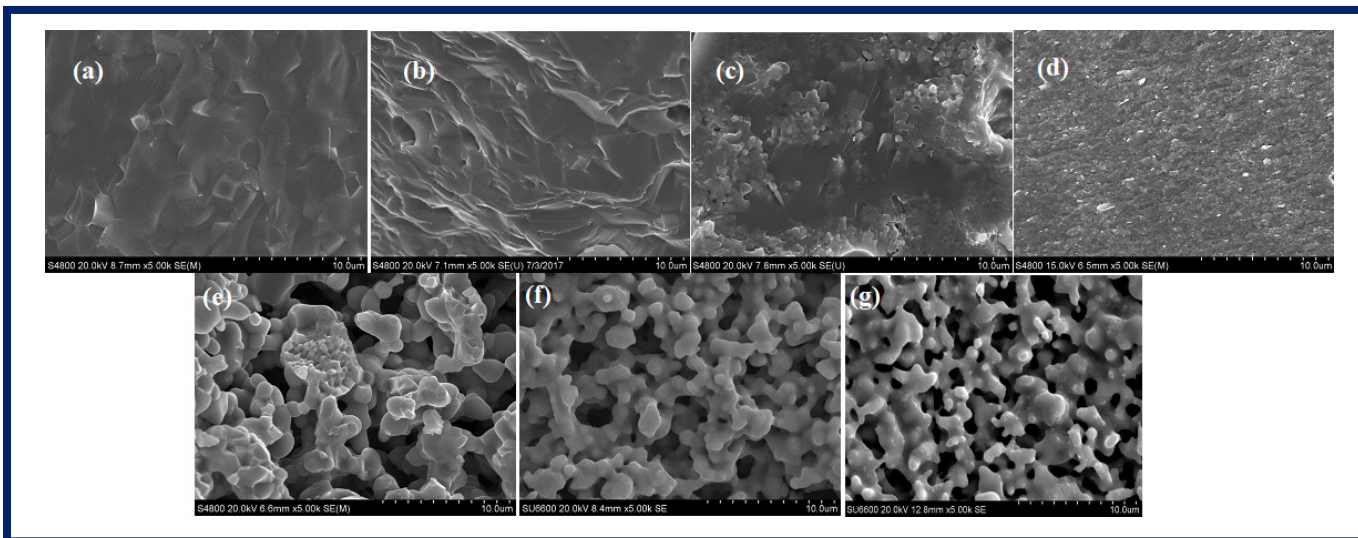


Fig. 6. Summary of the XRD patterns of protonic ceramic parts prepared by the RLRS method. (Adapted from Fig. 2 in Reference 51 (open access).)



**FIG. 7.** Summary of SEM images of fractured cross-sections of protonic ceramic component films prepared by the RLRS method. (a) BCZYYb+1wt%NiO electrolyte, (b) BZY20+1wt%NiO electrolyte, (c) LSC interconnector film, (d) BCF composite film, (e) 40wt%BCZYYb+60wt%NiO anode, (f) BCZY63 cathode scaffold, and (g) BCFZY0.1 cathode. (Adapted from Fig. 3 and Fig. 4 in Reference 51 (open access).)

the representative protonic ceramics of electrolyte, anode, cathode scaffold, cathode, interconnector, and hydrogen-permeable membrane. The protonic ceramic electrolyte films such as BCZYYb+1wt%, BZY20+1wt%NiO, the LSC interconnector, and the BCF hydrogen-permeable membrane obtained by RLRS are all fully dense. With good control of the laser parameters, the 40wt%BCZYYb+60wt%NiO anode, BCFZY0.1 cathode, and BCZY63 cathode scaffold films demonstrated highly porous microstructures.

Furthermore, the RLRS method demonstrated the capability to sinter the top layer of the protonic ceramics parts selectively. Figure 8a indicates that the dense BCZYYb electrolyte could be deposited on a pre-fabricated porous BCZYYb + Ni(O) anode substrate, which allowed the independently optimize the microstructures of the electrolyte and anode.<sup>53</sup> Figure 8b indicates that the RLRS could achieve the fully dense BCZYYb electrolyte on a porous BCZYYb layer by a single laser scan of the thick BCZYYb film. The vertical temperature distribution caused by the limited laser beam penetration made this fabrication of graded microstructure possible.<sup>50</sup> Figure 8c indicates that one-step RLRS could also fabricate the half cell consisting of BCZYYb+NiO anode and BCZYYb electrolyte due to vertical temperature distribution<sup>51</sup>.

In summary, the RLRS made it possible to process the component layers of the PCECCs with the desired crystal structures, microstructures, and geometries within instant time, which provides the potential to manufacture PCECCs and other ceramic devices using the rapid additive manufacturing technique. The selective sintering

of specific locations not only improve the processability but also significantly lower the processing cost. The capability to control the microstructures by controlling laser operation parameters and protonic ceramic precursor composition makes it possible to fabricate PCECCs.

## Integrated Additive Manufacturing and Laser Processing

Although recently, the PCECCs have achieved the promising device performance at intermediate-temperature (400-700°C), most of those excellent results were from the limited-scale devices (e.g., button cell  $\leq 1.0 \text{ cm}^2$ ) due to the limitation of manufacturing techniques. The novel additive manufacturing (AM) technology starts from designing 3D models of the objects by computer-aided design (CAD) software and then slices the models to successive cross-sectional layers. After that, the AM machines deposit these slices together to build the parts in a layer-by-layer fashion. Recently, the most successful examples focus on the manufacturing of polymers and metals/metal alloys because of the easiness and rapidness of consolidation or sintering of these materials. Although the AM of ceramics has also caught increasing attention, the successful AM of ceramic devices must solve the difficulty for achieving high accuracy due to the significant shrinkage, the difficulty for fulfilling crack-free rapid sintering due to the intrinsic brittleness, and the difficulty for depositing precise layers due to the heavy involvement of additive materials.

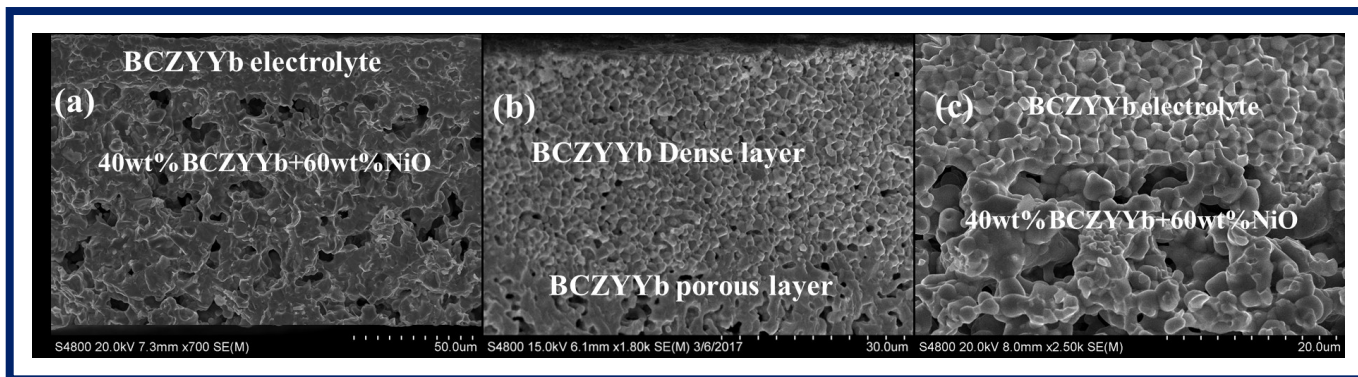


**FIG. 8.** SEM images of protonic ceramic half cells fabricated by using the RLRS method. (a) Independently RLRS deposition of BCZYYb electrolyte dense layer on the preprepared porous anode pellet, (b) one-step RLRS scanning of a thick BCZYYb film to prepare dense electrolyte layer on porous electrode scaffold, and (c) one-step RLRS scanning of a BCZYYb electrolyte | BCZYYb + NiO anode half cells. (Adapted from Fig. 2e in Reference 50 (open access), Fig. 5a in Reference 51 (open access), and Fig. 5e in Reference 53 with copyright permission.)

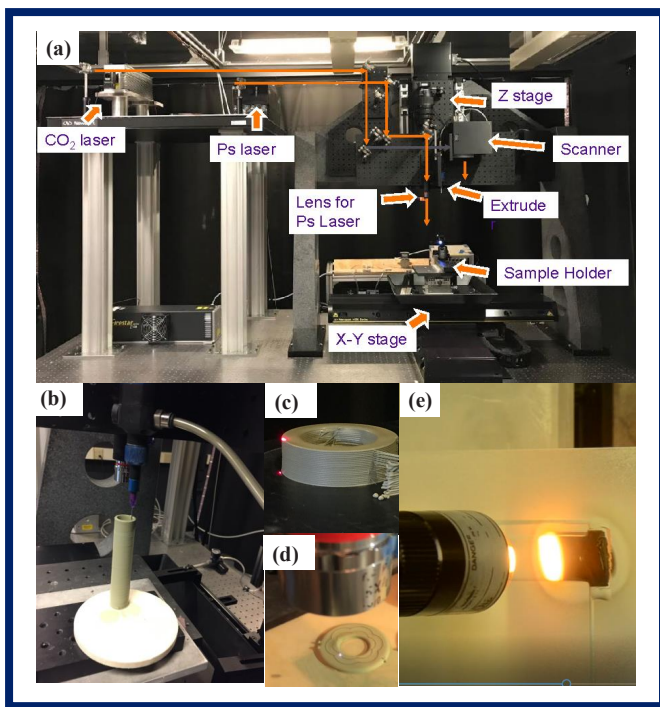


**FIG. 9.** I-AMLP system for the advanced manufacturing of ceramics. (a) Photo of I-AMLP system, (b) 3D printing based on microextrusion, (c) rapid laser drying during 3D printing, (d) rapid laser machining during 3D printing, and (e) rapid laser sintering of green layer. (Adapted from Fig. 1 in Reference 54 (open access).)

The recently developed RLRS technique allowed the possibility to utilize AM technology for the manufacturing PCECCs. Tong et al. developed a new integrated additive manufacturing and laser processing (I-AMLP) technique at Clemson University to process protonic ceramics.<sup>54</sup> The house-made I-AMLP station (Fig. 9a) consists of X-Y and Z stages, microextruders, a CO<sub>2</sub> laser, a picosecond YAG laser, and a Galvano scanner. The I-AMLP system can perform advanced manufacturing of green or sintered ceramic parts smoothly by combining the 3D printing based on fast microextrusion (Fig. 9b), accurate subtractive manufacturing based on laser processing (Fig. 9d), and in-situ consolidation based on high-energy laser sintering (Fig. 9e) and laser fast drying (Fig. 9c).

As summarized in Fig. 10, Tong et al. have shown that the I-AMLP method could work with the green and sintered protonic ceramic parts for intermediate-temperature protonic ceramic devices with various complex geometries and controlled microstructures. As a demonstration, the protonic ceramic pellets, cylinders, cones, rings, straight tubes with either closed bottom or top, and lobed-tube with closed bottom were successfully printed using the printable paste developed by us. NiO-BZY20 and NiO-BCZY0.1 anode, BZY20, BCZY0.1 electrolytes, triple conducting BCFZY0.1 oxygen/water permeable membrane materials, and BCF hydrogen-permeable composite membrane materials were involved. The effectiveness of laser drying, laser cutting, laser polishing, and laser sintering was demonstrated. Protonic ceramic parts of the 40wt% BZY20+6wt% NiO | BZY20+1wt% NiO tubular half cells, the BCFZY0.1 microchannel membrane, and the planar 40wt%BCZY0.1 + 60wt%NiO | BCZY0.1 + 1wt% half cells were successfully prepared.

Therefore, we can conclude that the newly developed I-AMLP provided an effective advanced manufacturing technique for rapidly and cost-effectively manufacturing PCECCs, which has a significant commercial future. The same method can also be utilized for the manufacturing of ceramic devices, especially for those devices with complicated geometry or multilayer and multifunctions.

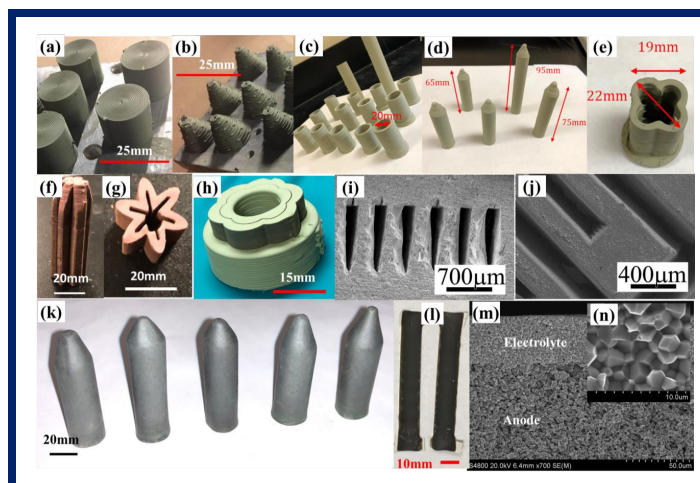


**FIG. 10.** Summary of the images or microstructures of green and sintered protonic ceramic parts manufactured by I-AMLP. (a) Green anode cylinders, (b) green anode cones, (c) green anode tubes with closed bottom end, (d) green anode with closed top end, (e) green anode tube with four lobes and closed bottom end, (f) green BCF tube with eight lobes introduced by laser cutting, (g) green BCF tube with eight lobes introduced by laser cutting, (h) short green anode co-axial tubes with lobes introduced by laser cutting, (i) and (j) sintered BCFZY0.1 membrane with embedded microchannels, (k) sintered protonic ceramic half cells fabricated by microextrusion-based AM process followed by coating and sintering, (l) half cells fabricated by one-step RLRS method, (m) SEM image of the fractured cross-section of the half cells shown in (l), and the high-magnification SEM image of the electrolyte shown in (m). (Adapted from Fig. 3, Fig. 6a, c, d, Fig. 7a, and Fig. 8a, b in Reference 54 (open access).)

## Future Direction

The recent progress of manufacturing techniques for PCECCs such as SSRS, RLRS, and I-AMLP provided the possibility to rapidly and cost-effectively manufacture PCECCs on a large scale. The fundamental understanding of the mechanisms why these methods worked well need to be understood for further improving the method and expanded their applications to other materials systems. The demonstration of the I-AMLP for manufacturing PCECC stacks needs to contribute more effort. The understanding of the laser beam and materials need to be further pursued for providing manufacturing guidance. The new efficient design of PCECC devices can move further since the technique for manufacturing complicated and multifunctional ceramics becomes possible.

## Acknowledgements

This material is based upon work supported by the U.S. Department of Energy's Office of Energy Efficiency and Renewable Energy (EERE) under the Hydrogen and Fuel Cell Technologies Office Award Number DE-EE0008428.

## Disclaimer

“This report was prepared as an account of work sponsored by an agency of the United States Government. Neither the United States Government nor any agency thereof, nor any of their employees, makes any warranty, express or implied, or assumes any legal liability or responsibility for the accuracy, completeness, or usefulness of any information, apparatus, product, or process disclosed, or represents that its use would not infringe privately owned rights. Reference herein to any specific commercial product, process, or service by trade name, trademark, manufacturer, or otherwise does not necessarily constitute or imply its endorsement, recommendation, or favoring by the United States Government or any agency thereof. The views and opinions of authors expressed herein do not necessarily state or reflect those of the United States Government or any agency thereof.”

© The Electrochemical Society. DOI: 10.1149/2.2.F09204IF.

(continued on next page)

## About the Authors



**SHENGLONG MU** is a PhD student from Dr. Tong's group in materials science and engineering at Clemson University. Shenglong received his MS in polymer engineering from The University of Akron in May 2016 and his BS in materials science and engineering from the Beijing University of Chemical Technology. His main research interests focus on the study of reactive laser sintering and 3D printing of protonic ceramic energy devices. He also has experience

in the polymer drying process and uniaxial stretching investigation of polymer film. At Clemson, Shenglong is the first member of Dr. Tong's Sustainable Clean Energy Laboratory. He has focused on the development of new manufacturing techniques, additive manufacturing, and lasering processing for protonic ceramic energy devices. Shenglong has six first-authored papers published and 12 published papers in addition to one patent. He may be reached at [smu@g.clemson.edu](mailto:smu@g.clemson.edu).

<https://orcid.org/0000-0002-2191-7470>



**ZEYU ZHAO** received his BS and MS in materials science and engineering from the Beijing University of Chemical Technology in 2013 and 2016, respectively. He is currently in his fifth year as a PhD student in materials science and engineering with Dr. Tong at Clemson University. His research interests focus on developing dual-phase or multi-phase materials for energy devices, especially for protonic ceramic fuel cells, and the investigation of ionic conducting properties inside

of these materials. He may be reached at [zzhao2@g.clemson.edu](mailto:zzhao2@g.clemson.edu).

<https://orcid.org/0000-0001-8649-925X>



**HUA HUANG** is a postdoctoral researcher of materials science and engineering at Clemson University. His research interests focus on 3D printing integrated with laser rapid sintering processing for protonic ceramic fuel cells and electrolyzers. He also has rich experience in dual-phase oxygen separation membrane reactor and phase-inversion tape casting for ceramic devices fabrication. He received his BS in inorganic non-metal material engineering from Hefei University

of Technology in 2009, and a PhD in materials science and engineering from the University of Science and Technology of China in 2014. Before joining Clemson, he worked at the Technical University of Denmark, Risø National Laboratory, as a research assistant in 2013. From 2014 to 2018, he worked at the Institute of Nuclear Energy Safety Technology, Chinese Academy of Sciences, as an assistant researcher for nuclear hydrogen production. He may be reached at [hhuang8@clemson.edu](mailto:hhuang8@clemson.edu).

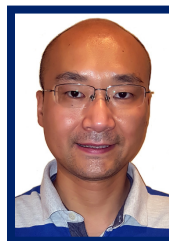
<https://orcid.org/0000-0002-6234-2327>



**JINCHENG LEI** is a postdoctoral research associate at Clemson University. He received a PhD degree in electrical engineering from Clemson University in 2019, and a bachelor's degree in materials science and engineering from the South China University of Technology, Guangzhou, China, in 2013. His research interest mainly focuses on design, development, and implementation of advanced manufacturing technologies to enable novel micro/nano materials, structures, devices,

and sensors for photonic and electronic applications. He may be reached at [jinchel@g.clemson.edu](mailto:jinchel@g.clemson.edu).

<https://orcid.org/0000-0003-1272-9555>



**FEI PENG** is an associate professor of materials science and engineering at Clemson University, and an affiliated faculty member of the Clemson University School of Health Research (CUSHR). He received his PhD from the Georgia Institute of Technology, and MS and BS from Tsinghua University. He has extensive training in ceramic processing, modeling, characterization, and testing. Dr. Peng is leading the advanced ceramic processing laboratory at MSE of Clemson

University. His research is focused on overcoming the processing challenges during additive manufacturing ceramics, such as extrusion, inkjet printing, and laser sintering and micromachining. He has made significant contributions to the laser sintering of ceramics and fabricating embedded microchannels within ceramics. Dr. Peng has published over 40 peer-reviewed journal papers. He may be reached at [fpeng@clemson.edu](mailto:fpeng@clemson.edu).

<https://orcid.org/0000-0002-3924-9028>



**HAI XIAO** is the Samuel Lewis Bell Distinguished Professor of Electrical and Computer Engineering, and professor of bioengineering, at Clemson University. From 2006 to 2013, he was associate professor, then professor of electrical engineering, at the Missouri University of Science and Technology, where he also served as the founding director of the Photonics Technology Laboratory. From 2003 to 2006, he was an assistant professor of electrical engineering at the

New Mexico Institute of Mining and Technology. From 2000 to 2003, he was a member of the technical staff at the Optoelectronic Center of Lucent Technologies/Agere Systems. Dr. Xiao received his PhD in electrical engineering from Virginia Tech in 2000. Dr. Xiao is the recipient of a number of prestigious awards, including the Office of Naval Research Young Investigator Program Award in 2006, and the R&D 100 Award in 2004. Dr. Xiao's research interests mainly focus on sensors, instrumentation, materials, systems, and advanced manufacturing technologies for applications in energy, intelligent infrastructure, clean environment, biomedical sensing/imaging, and national security. Dr. Xiao has authored and coauthored over 160 journal papers and served as the principal investigator or co-investigator for over 40 research projects. He may be reached at [haix@clemson.edu](mailto:haix@clemson.edu).

ORCID iD: <https://orcid.org/0000-0003-1460-6241>




**KYLE S. BRINKMAN** is the chair of the Department of Materials Science and Engineering at Clemson University. He received a BS in chemical engineering in 1998 and MS in materials science and engineering in 2000, both from Clemson. In 2004, he graduated from the Swiss Federal Institute of Technology in Lausanne, Switzerland, with a PhD in materials science and engineering. From 2005-2007, Brinkman served as a postdoctoral fellow at the National Institute of

Advanced Industrial Science and Technology in Japan as part of a program sponsored by the Japan Society for the Promotion of Science. He later worked as a principal engineer in the Science and Technology Directorate of the U.S. Department of Energy's Savannah River National Laboratory from 2007-2014. Brinkman joined Clemson as an associate professor in 2014. He has authored or coauthored more than 100 peer-reviewed technical publications and government reports, three patents, and currently serves as an editor for the *Journal of Materials Science*. He is codirector of Clemson's Nuclear Environmental Engineering Sciences and Radioactive Waste Management Center. Brinkman was the recipient of the Minerals, Metals and Materials Society (TMS) Young Leader International Scholar Award (2015), and the TMS Brimacombe Medalist Award (2020). He was elected a Fellow of the American Ceramic Society in 2020, and is the vice-chair of the Energy Materials and Systems Division. In 2015, he was awarded the Karl Schwartzwalder Professional Achievement in Ceramic Engineering Award. Brinkman's




research is related to the formation, structure, and behavior of ceramic composites in diverse application areas, including solid oxide fuel cells and ionic membrane systems, solid state lithium batteries, and ceramics for nuclear waste immobilization. He may be reached at ksbrink@clemsun.edu.

 <https://orcid.org/0000-0002-2219-1253>



**JIANHUA (JOSHUA) TONG** is an associate professor of materials science and engineering at Clemson University. Before joining Clemson in 2016, he was a research assistant/associate professor at the Colorado School of Mines. At Clemson, Dr. Tong manages the Sustainable Clean Energy Laboratory. He has published more than 80 peer-reviewed papers and six book chapters, and filed 15 patents. His publications have been cited over 5,200 times, and his h-index

is greater than 33. He received his PhD from the Dalian Institute of Chemical Physics, CAS. In addition, he received extensive researcher/JSPS fellow/postdoc training on catalytic membrane reactors and solid oxide fuel cells at the Research Institute of Innovative Technology for the Earth, the National Institute of Advanced Industrial Science and Technology, the University of Cincinnati, and the California Institute of Technology. He may be reached at jianhut@clemsun.edu.

 <https://orcid.org/0000-0002-0684-1658>

## References

- H. Iwahara, T. Esaka, H. Uchida, and N. Maeda, N., *Solid State Ionics*, **3-4**, 359 (1981).
- H. Iwahara, H. Uchida, and N. Maeda, *Solid State Ionics*, **11**, 109 (1983).
- C. C. Duan, J. H. Tong, M. Shang, S. Nikodemski, M. Sanders, S. Ricote, A. Almansoori, R. O'Hayre, *Science*, **349**, 1321 (2015).
- L. Yang, S. Z. Wang, K. Blinn, M. F. Liu, Z. Liu, Z. Cheng, and M. L. Liu, *Science*, **326**, 126 (2009).
- S. Choi, C. J. Kucharczyk, Y. G. Liang, X. H. Zhang, I. Takeuchi, H. I. Ji, and S. M. Haile, *Nat. Energy*, **3**, 202 (2018).
- H. An, H. W. Lee, B. K. Kim, J. W. Son, K. J. Yoon, H. Kim, D. Shin, H. I. Ji, and J. H. Lee, *Nat. Energy*, **3**, 870 (2018).
- C. C. Duan, R. J. Kee, H. Y. Zhu, C. Karakaya, Y. C. Chen, S. Ricote, A. Jarry, E. J. Crumlin, D. Hook, R. Braun, N. P. Sullivan, and R. O'Hayre, *Nature*, **557**, 217 (2018).
- J. M. Serra, *Nat. Energy*, **4**, 178 (2019).
- C. C. Duan, R. Kee, H. Y. Zhu, N. Sullivan, L. Z. Zhu, L. Z. Bian, D. Jennings, and R. R. O'Hayre, *Nat. Energy*, **4**, 230 (2019).
- S. Choi, T. C. Davenport, and S. M. Haile, *Energy Environ. Sci.*, **12**, 206 (2019).
- S. H. Morejudo, R. Zanon, S. Escolastico, I. Yuste-Tirados, H. Malerod-Fjeld, P. K. Vestre, W. G. Coors, A. Martinez, T. Norby, J. M. Serra, and C. Kjolseth, *Science*, **353**, 563 (2016).
- H. Iwahara, *Solid State Ionics*, **86-8**, 95 (1996).
- K. D. Kreuer, *Annu. Rev. Mater. Res.*, **33**, 333 (2003).
- W. A. Meulenber, M. E. Ivanova, J. M. Serra, and S. Roitsch, in *Advanced Membrane Science, and Technology for Sustainable Energy and Environmental Applications*, p. 541, Woodhead Publishing, Cambridge (2011).
- J. Kim, S. Sengodan, S. Kim, O. Kwon, Y. Bu, and G. Kim, *Renewable Sustainable Energy Rev.*, **109**, 606 (2019).
- Y. Q. Meng, J. Gao, Z. Y. Zhao, J. Amoroso, J. H. Tong, and K. S. Brinkman, *J. Mater. Sci.*, **54**, 9291 (2019).
- C. C. Duan, J. K. Huang, N. Sullivan, and R. O'Hayre, *Appl. Phys. Rev.*, **7**, 011314 (2020).
- N. Taniguchi, K. Hatoh, J. Niikura, T. Gamou, and H. Iwahara, *Solid State Ionics*, **53**, 998 (1992).
- K. D. Kreuer, *Solid State Ionics*, **97**, 1 (1997).
- K. H. Ryu and S. M. Haile, *Solid State Ionics*, **125**, 355 (1999).
- H. Wang, R. R. Peng, X. F. Wu, J. L. Hu, and C. R. Xia, *J. Am. Ceram. Soc.*, **92**, 2623 (2009).
- S. Nikodemski, J. H. Tong, C. C. Duan, and R. O'Hayre, *Solid State Ionics*, **294**, 372 (2016).
- C. Antonio Goulart, L. A. V. B., Márcio Raymundo Morelli, Dulcinea Pinatti Ferreira de Souza, *Ceram. Int.*, <https://doi.org/10.1016/j.ceramint.2020.09.102> (2020).
- E. Fabbri, A. D'Epifanio, E. Di Bartolomeo, S. Licocchia, and E. Traversa, *Solid State Ionics*, **179**, 558 (2008).
- S. W. Tao and J. T. S. Irvine, *J. Solid State Chem.*, **180**, 3493 (2007).
- Y. Yamazaki, R. Hernandez-Sanchez, and S. M. Haile, *J. Mater. Chem.*, **20**, 8158 (2010).
- R. B. Cervera, Y. Oyama, S. Miyoshi, K. Kobayashi, T. Yagi, and S. Yamaguchi, *Solid State Ionics*, **179**, 236 (2008).
- P. Babilo, T. Uda, and S. M. Haile, *J. Mater. Res.*, **22**, 1322 (2007).
- C. Peng, J. Melnik, J. L. Luo, A. R. Sanger, and K. T. Chuang, *Solid State Ionics*, **181**, 1372 (2010).
- D. Pergolesi, E. Fabbri, A. D'Epifanio, E. Di Bartolomeo, A. Tebano, S. Sanna, S. Licocchia, G. Balestrino, and E. Traversa, *Nat. Mater.*, **9**, 846 (2010).
- Y. Yamazaki, R. Hernandez-Sanchez, and S. M. Haile, *Chem. Mater.*, **21**, 2755 (2009).
- H. Bae and G. M. Choi, *J. Power Sources*, **285**, 431 (2015).
- S. W. Wang, Y. Chen, L. L. Zhang, C. Ren, F. L. Chen, and K. S. Brinkman, *J. Electron. Mater.*, **44**, 4898 (2015).
- S. W. Wang, Y. F. Liu, J. He, F. L. Chen, and K. S. Brinkman, *Int. J. Hydrogen Energy*, **40**, 5707 (2015).
- P. Babilo and S. M. Haile, *J. Am. Ceram. Soc.*, **88**, 2362 (2005).
- B. Lin, Y. C. Dong, S. L. Wang, D. R. Fang, H. P. Ding, X. Z. Zhang, X. Q. Liu, and G. Y. Meng, *J. Alloys Compd.*, **478**, 590 (2009).
- J. H. Tong, D. Clark, M. Hoban, and R. O'Hayre, *Solid State Ionics*, **181**, 496 (2010).
- J. H. Tong, D. Clark, L. Bernau, A. Subramanian, and R. O'Hayre, *Solid State Ionics*, **181**, 1486 (2010).
- S. Nikodemski, J. H. Tong, and R. O'Hayre, *Solid State Ionics*, **253**, 201 (2013).
- S. Ricote and Bonanos, *Solid State Ionics*, **181**, 694 (2010).
- D. Clark, J. Tong, A. Morrissey, A. Almansoori, I. Reimanis, and R. O'Hayre, *Phys. Chem. Chem. Phys.*, **16**, 5076 (2014).
- S. Ricote, N. Bonanos, A. Manerbin, and W. G. Coors, *Int. J. Hydrogen Energy*, **37**, 7954 (2012).
- J. F. Bu, P. G. Jonsson, and Z. Zhao, *J. Power Sources*, **272**, 786, (2014).
- S. M. Choi, J. H. Lee, J. Hong, H. Kim, K. B. Yoon, B. K. Kim, and J. H. Lee, *Int. J. Hydrogen Energy*, **39**, 7100 (2014).
- Y. G. Meng, J. Gao, H. Huang, M. D. Zou, J. Duffy, J. H. Tong, and K. S. Brinkman, *J. Power Sources*, **439**, 227093 (2019).
- Z. Y. Zhao, J. Cui, M. D. Zou, S. L. Mu, H. Huang, Y. Q. Meng, K. He, K. S. Brinkman, and J. H. Tong, *J. Power Sources*, **450**, 22769 (2020).
- S. Escolastico, M. Ivanova, C. Solis, S. Roitsch, W. A. Meulenber, and J. M. Serra, *RSC Adv.*, **2**, 4932 (2012).
- S. M. Fang, S. W. Wang, K. S. Brinkman, and F. L. Chen, *J. Mater. Chem., A*, **2**, 5825 (2014).
- W. A. Rosensteel, S. Ricote, and N. P. Sullivan, *Int. J. Hydrogen Energy*, **41**, 2598 (2016).
- S. L. Mu, Z. Y. Zhao, J. C. Lei, Y. Z. Hong, T. Hong, D. Jiang, Y. Song, W. Jackson, K. S. Brinkman, F. Peng, H. Xiao, and J. H. Tong, *Solid State Ionics*, **320**, 369 (2018).
- S. L. Mu, H. Huang, A. Ishii, Y. Z. Hong, A. Santomauro, Z. Y. Zhao, M. D. Zou, F. Peng, K. S. Brinkman, H. Xiao, and J. H. Tong, *ACS Omega*, **5**, 11637 (2020).
- A. Ishii, S. L. Mu, Y. Q. Meng, H. Huang, J. C. Lei, Y. J. Li, F. Peng, H. Xiao, J. H. Tong, and K. S. Brinkman, *Energy Technol.*, DOI: 10.1002/ente.202000364 (2020).
- H. H. Shenglong Mu, A. Ishii, Z. Zhao, M. Zou, P. Kuzbary, F. Peng, K. S. Brinkman, H. Xiao, and J. Tong, *J. Power Sources Advances*, **4**, 1000172 (2020).
- S. L. Mu, Y. Z. Hong, H. Huang, A. Ishii, J. C. Lei, Y. Song, Y. J. Li, K. S. Brinkman, F. Peng, H. Xiao, and J. H. Tong, *Membranes*, **10**, 98 (2020).